Analytical Solution of Free Radical Polymerization: Applications–Implementing Nonisothermal Effect

6 AUTHORS, INCLUDING:

Dhiraj Kumar Garg

Shiv Nadar University

12 PUBLICATIONS   49 CITATIONS

SEE PROFILE

Christophe A Serra

University of Strasbourg

104 PUBLICATIONS   1,272 CITATIONS

SEE PROFILE

Yannick Hoarau

University of Strasbourg

69 PUBLICATIONS   354 CITATIONS

SEE PROFILE

Dambarudhar Parida

University of Bordeaux

13 PUBLICATIONS   55 CITATIONS

SEE PROFILE

Analytical Solution of Free Radical Polymerization: Applications-Implementing Nonisothermal Effect

Dhiraj K. Garg,[†,§] Christophe A. Serra,*[,‡,§] Yannick Hoarau,[†] Dambarudhar Parida,[‡] M. Bouquey,[‡,§] and R. Muller[‡,§]

[†]Laboratoire des Sciences de l'Ingénieur, de l'Informatique et de l'Imagerie (ICUBE), Université de Strasbourg (UdS), F-67000 Strasbourg, France

[‡]École Européenne de Chimie, Polymères et Matériaux (ECPM), Université de Strasbourg (UdS), 25 rue Becquerel, F-67087 Strasbourg Cedex 2, France

[§]Institut Charles Sadron (ICS)—UPR 22 CNRS, 23 rue du Loess, F-67034 Strasbourg Cedex 2, France

S *Supporting Information*

ABSTRACT: Analytical solution (AS), as derived in our previous works for isothermal free radical polymerization (FRP), has been extended to nonisothermal conditions in this work. Only one differential equation, i.e., the energy balance equation, was required to calculate temperature profile by stiff solver using AS as input values. The results were compared against numerical solution (NS) of the complete set of ordinary differential equations (ODE) of FRP, 11 ODE for full set of equations (FRP_Full), and 8 ODE for quasi steady state approximation (FRP_QSSA). Two different models, namely Chiu, Carratt, and Soong (CCS) and Achilias and Kiparissides (AK), for implementing the gel/glass/cage effect, were also considered. The results were validated against published results and were found to be in excellent agreement, as well as with NS for all conditions taken. This work proved the versatility, flexibility, and adaptability of AS under all conditions (except for low temperatures) and with various models to simulate gel/glass/cage effect along with nonisothermal conditions.
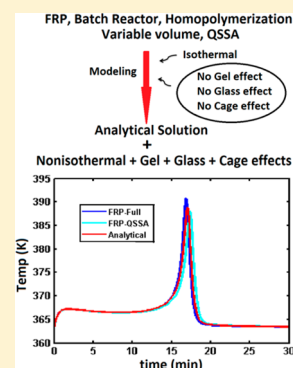
INTRODUCTION

One of the key requirements to control exothermic and endothermic reactions is the strict management of temperature. Indeed, in first place, temperature affects kinetic rate coefficients of different reaction paths through their activation energy. Higher temperature usually increases rates of exothermic reactions and thus decreases reaction time to reach a given conversion. The beneficial consequence is an increase in productivity or space time yield for continuous flow reactors. But depending on the reaction type, this increase in temperature may trigger unwanted side reactions, changes phase equilibrium, affects reactants and products solubility and so on. This can limit the temperature range of operation. Temperature rise may also be required to reduce the viscosity of the reaction mixture to reduce pumping power especially in the case of polymers. In many exothermic reactions, loss of temperature control may lead to thermal runaways in the absence of an appropriate heat sink capacity. This is quite detrimental to the safety, maintenance and plant operation. Temperature variations may also lead to the formation of wide range of side products thus degrading the overall quality of the desired product.

Polymerization reactions are one such type of reactions where temperature and its control play a very vital role in controlling the quality of the product. Unlike other reaction types, conversion is not the most important parameter here. One of the important characteristics of the polymerization reaction is to produce product having number-average molecular weight (MW_n), polydispersity index (PDI), branching etc. in a narrow specified range. Otherwise, the product may be useless for the desired application(s).

Various thermophysical properties of polymers are strong function of temperature. So in some cases, even small temperature changes may lead to large variation in the product quality. During reaction, these temperature variations may occur due to improper mixing, poor cooling/heating arrangement etc. combined with exothermic nature of polymerization reactions. There are various phenomena interrelated with temperature in case of polymerization. Polymer reaction mixture viscosity increases almost exponentially with conversion, so to handle and properly mix such a highly viscous fluid, large mechanical power is required which in turn may contribute to increase the temperature by viscous dissipation. To reduce this power, a higher temperature is desirable so as to reduce the viscosity. Another way of reducing viscosity could be the addition of some solvent to the reaction mixture. But this option may be limited by the product specification requirement as well as the downstream solvent separation and recovery processes. Inefficient solvent separation process may deteriorate the quality of the product and inefficient solvent recovery

processes may make the operation uneconomical. By increasing the temperature, one can increase the polymerization rate, but it also increases the decomposition of initiator, especially in the case of free radical polymerization (FRP) initiated by thermal activation of the initiator. This may lead to the situation of incomplete conversion due to the rapid initiator decomposition.[1] This problem can be overcome by adding more initiator, but it significantly decreases the molecular weight. So we have a trade-off.

It would always be helpful if there is some study which can help in predicting such undesirable conditions and their outcome beforehand. The same study could also be used to search for optimum temperature and other parameters values that would optimize the product quality and production rate. Most of the experimental data and numerical solution (NS) available are obtained under isothermal conditions.[2−7] Very less research has been done in the field of nonisothermal behavior of polymerization reactions. Baillagou and Soong[1,8] had done one such study. But their study was numerical. They had used Chiu, Carratt, and Soong[9] (CCS) method for implementing gel/glass effect. They had been able to show various practical aspects of temperature variation under various conditions like different heat sink temperature, initiator concentration, overall heat transfer coefficient, and solvent fraction. They had studied the molecular weight distribution, conversion and temperature variation in all such combinations of situations.

Ray et al.[10] and Srinivas et al.[11] had studied experimentally the stepwise variation in reaction temperature. They had also developed a mathematical model using CCS model with free volume theory. But this model was semi- theoretical in nature as they had used best fit correlations to match the experimental data. They performed the step increase and step decrease of temperature at two different times each. They validated their modeling results with experimental data. Sangwai et al.[12] had also performed similar work but with an empirical mathematical model with best fit correlations.

Venkateshwaran et al.[13] had done such nonisothermal study too, using the analytical solution (AS) they had derived and tried to compare the results of AS and NS for isothermal and nonisothermal condition with and without gel conditions. They had used the CCS model for implementing the gel/glass effect. All this was done for constant volume condition. Their match of AS with NS was not that good, and the AS they derived was quite complicated, cumbersome, and lengthy.
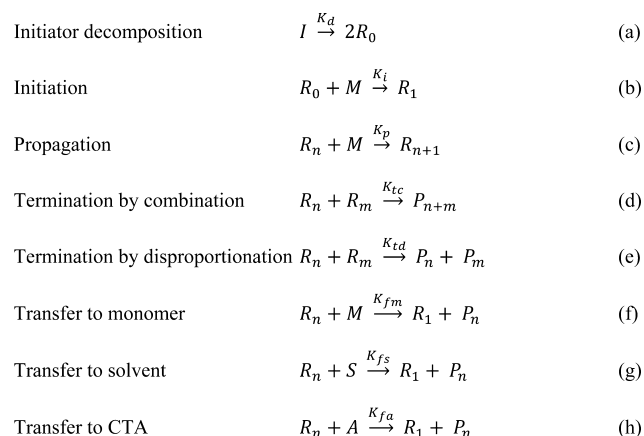
We had derived AS of the free radical polymerization in our previous work[14] for isothermal, homogeneous, bulk/solution, without gel effect, variable volume batch reactor. We later extended our work[15] to implement the gel and glass effect using the CCS model. We then further improved our AS[16] by replacing it with the Achilias and Kiparissides[17] (AK) model which incorporates the CCS model with free volume theory for diffusion coefficients for monomer, polymer, and initiator. All these previous works were done at constant temperature. The key objective of this work is to present the implementation of nonisothermal effects in AS we had obtained in our previous work. The current work demonstrates the complete versatility of AS with respect to changes in temperature, kinetic rate co-efficients and initiator efficiency. The results were obtained for (1) no gel/glass/cage effect, (2) with gel/glass effect with the CCS model, and (3) with gel/glass/cage effect using the AK model. AS results are then compared with the respective NSs. They were also validated against published numerical results.[1,8]

■ THEORY

1. Reaction Mechanism and Kinetic Equations. Scheme 1 is adopted, the same as in our previous work:[14]

Scheme 1. Kinetic Scheme of FRP Considered for the Study

Initiator decomposition	$I \xrightarrow{K_d} 2R_0$	(a)
Initiation	$R_0 + M \xrightarrow{K_i} R_1$	(b)
Propagation	$R_n + M \xrightarrow{K_p} R_{n+1}$	(c)
Termination by combination	$R_n + R_m \xrightarrow{K_{tc}} P_{n+m}$	(d)
Termination by disproportionation	$R_n + R_m \xrightarrow{K_{td}} P_n + P_m$	(e)
Transfer to monomer	$R_n + M \xrightarrow{K_{fm}} R_1 + P_n$	(f)
Transfer to solvent	$R_n + S \xrightarrow{K_{fs}} R_1 + P_n$	(g)
Transfer to CTA	$R_n + A \xrightarrow{K_{fa}} R_1 + P_n$	(h)

2. Mathematical Model of FRP. The mathematical model based on the moment method[14] is chosen for this kinetic scheme. The developed mathematical model is presented in Appendix A in the Supporting Information.

3. Summary of Analytical Solution in Time Step Format. The assumptions of isothermal, homogeneous, variable volume, without gel/glass effect, bulk/solution, and homopolymerization were used to derive AS. The details of the derivation of AS can be found in our previous work.[14] The summary of AS in time step form is given in Appendix B in the Supporting Information.

4. Constitutive Equations for the Gel and Glass Effect Using the CCS Model. All the equations used in this work are presented in Appendix C in the Supporting Information.

5. Constitutive Equations for the Cage, Gel, and Glass Effect Using Free Volume Theory. The details of the equations are given in Appendix D in the Supporting Information.

6. Physical and Chemical Data. The Physical and chemical used in this work is given in Appendix-E in the Supporting Information.

7. Methodology. The methodology developed here was same as the one adopted in our previous work.[14−16] We used the three sets of mathematical equations: FRP_Full, FRP_QSSA, and Analytical. FRP_Full consisted of equations given in Appendix A in the Supporting Information and hence represents the complete model without any additional assumption. FP_QSSA was obtained by applying the quasi steady state approximation (QSSA) on λ_0, λ_1, and λ_2 zeroth, first, and second orders of moment of live polymer chain length distributions, respectively. Thus, eqs B10−B12 with eqs B25 and B26 were obtained from eqs A6−A8. Analytical consisted of equation given in Appendix-B in the Supporting Information with eqs A14−A40 along with eq A12 for temperature. As the current mathematical models comprised of sets of stiff equations, stiff solver ode15s in Matlab R2008a was used for solving all the three sets. The FRP_Full is represented by blue, FRP_QSSA by green, and Analytical by red color in all the plots shown in all the figures in the Results.

All the variables were calculated at the beginning of each time step. Kinetic rate coefficients and initiator efficiency were
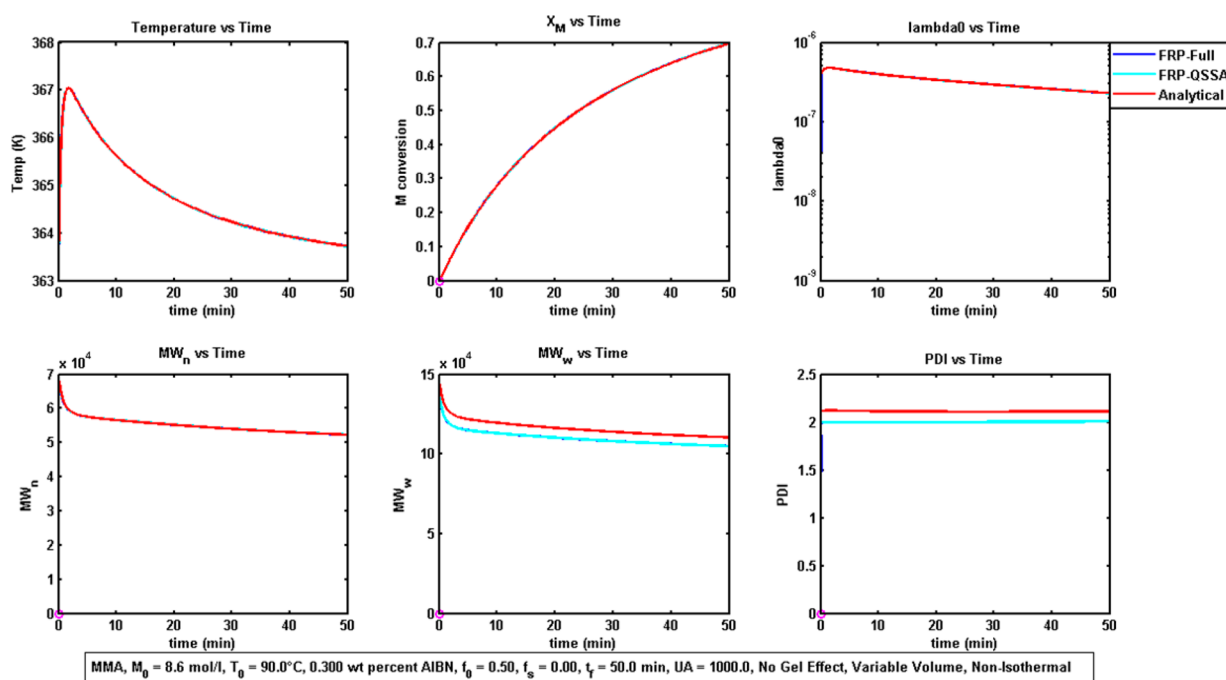
Figure 1. MMA: Results obtained for temperature variation with UA = 1000 cal/min/K for no gel/glass/cage effect.
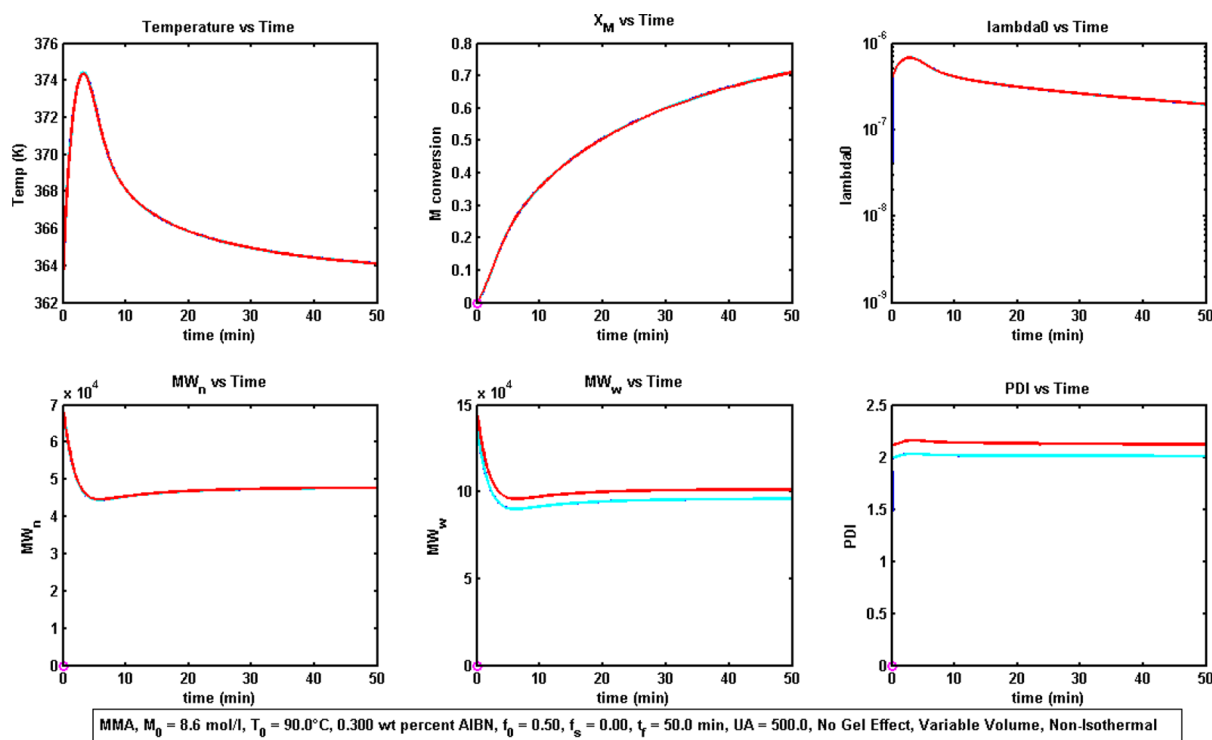

Figure 2. MMA: Results obtained for temperature variation with UA = 500 cal/min/K for no gel/glass/cage effect.

evaluated using the above presented models. For the analytical model, values obtained for various variables from AS were used in the temperature differential equation. This temperature differential equation was then solved using ode solver. For details of the methodology, please refer to our previous work.[14−16]

The results were obtained for the polymerization of methyl methacrylate (MMA) for which used physical and chemical properties are summarized in Table 1 in Appendix E in the Supporting Information. Two types of heat transfer cases were

considered: one with fixed heat transfer rate and the other one where heat transfer was neglected, i.e., the adiabatic condition. The latter case represented the worst condition from thermal point of view as all the heat released by the polymerization remained inside the reactor, leading to maximum temperature rise. The overall heat transfer coefficient U was taken along with heat transfer area A_H, i.e., UA to make the analysis independent of individual variations of U and A_H. The initial reaction temperature was taken to be 90 °C in all cases for the sake of simplicity. The heat sink temperature T_{bath} was taken to
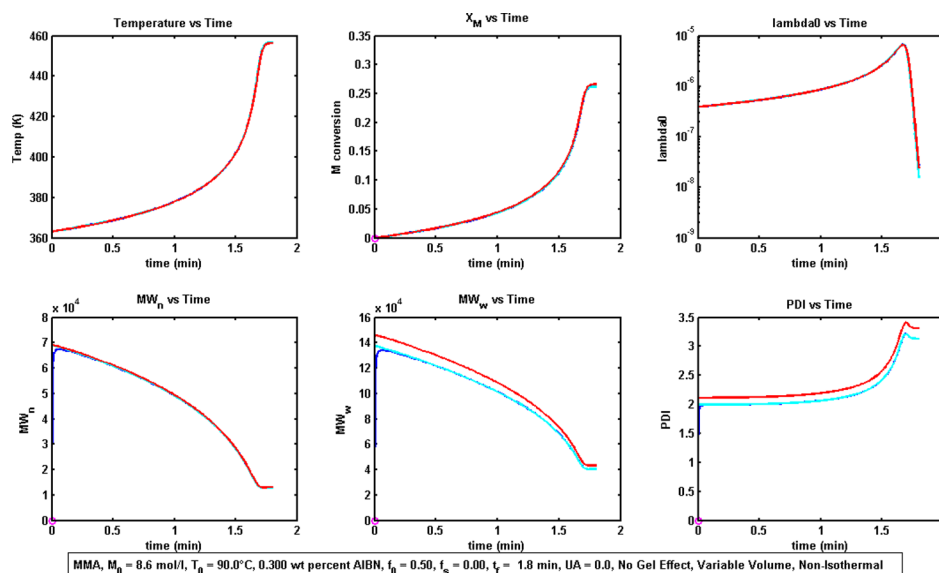
Figure 3. MMA: Results obtained for temperature variation with $UA = 0$ cal/min/K (adiabatic) for no gel/glass/cage effect.
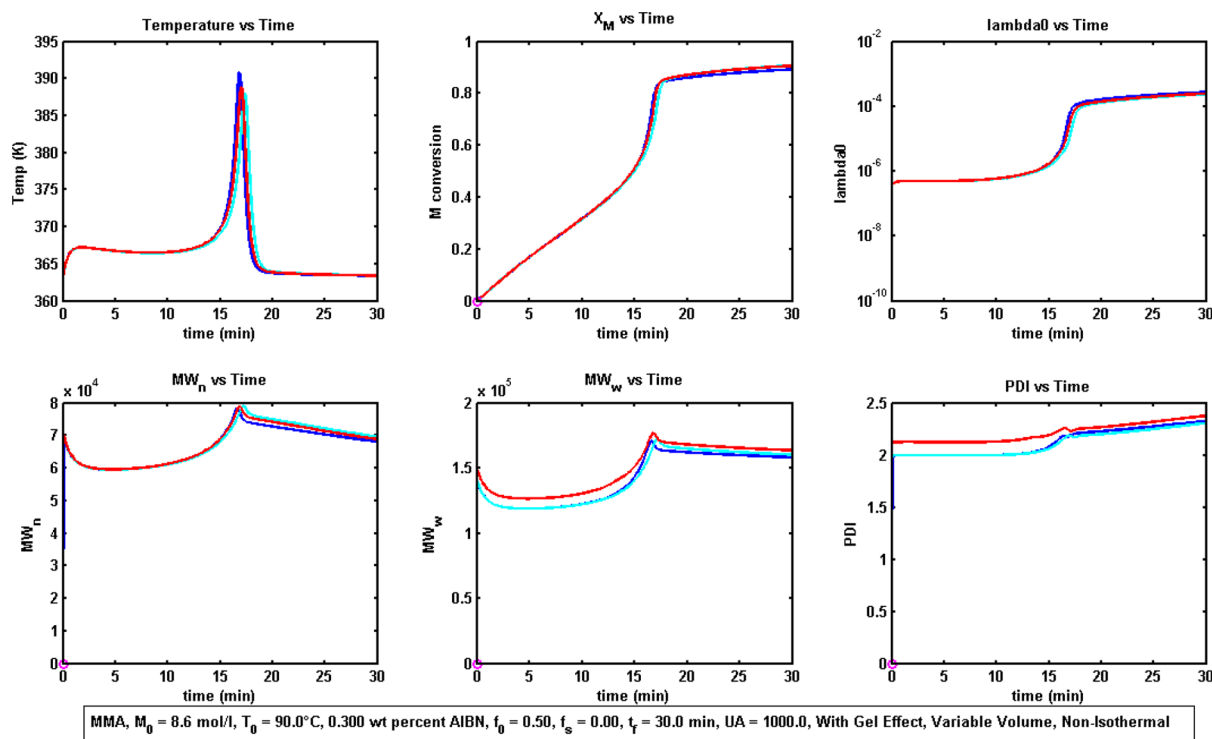

Figure 4. MMA: Results obtained for temperature variation with $UA = 1000$ cal/min/K for the gel/glass effect with the CCS model.

be the same as the initial reaction temperature to simulate isothermal conditions.

■ RESULTS

Figures 1−3 show the results for the condition without any gel/glass/cage effect with different heat transfer rates from $UA = 1000$ cal/min/K (Figure 1) to $UA = 500$ cal/min/K (Figure 2) to adiabatic condition for which $UA = 0$ cal/min/K (Figure 3). They clearly show that temperature profile predicted by AS matched excellently with NS in all cases. The match with other variables predicted is also good.

Figures 4−7 show the results for conditions implementing gel/glass effect using CCS model. Figures 4 and 5 show the

results for $UA = 1000$ cal/min/K whereas Figures 6 and 7 show the results for adiabatic condition. Figures 5 and 7 show the results for variation in K_t and K_{pr} with temperature change. f was held constant (no cage effect) in this model. It can be observed that here too, AS matches excellently with the NS predicted temperature profile and other variables.

Figures 8−11 show the results for the conditions implementing gel/glass and cage effect using the AK model. Figures 8 and 10 show the results for $UA = 5000$ cal/min/K whereas Figures 9 and 11 show the results for adiabatic condition. Figures 9 and 11 show the results for variation in K_t, K_{pr} and f with temperature changes. Again, the results for AS match well with NS for temperature profile as well as for all other variables as shown in Figures 1−11.
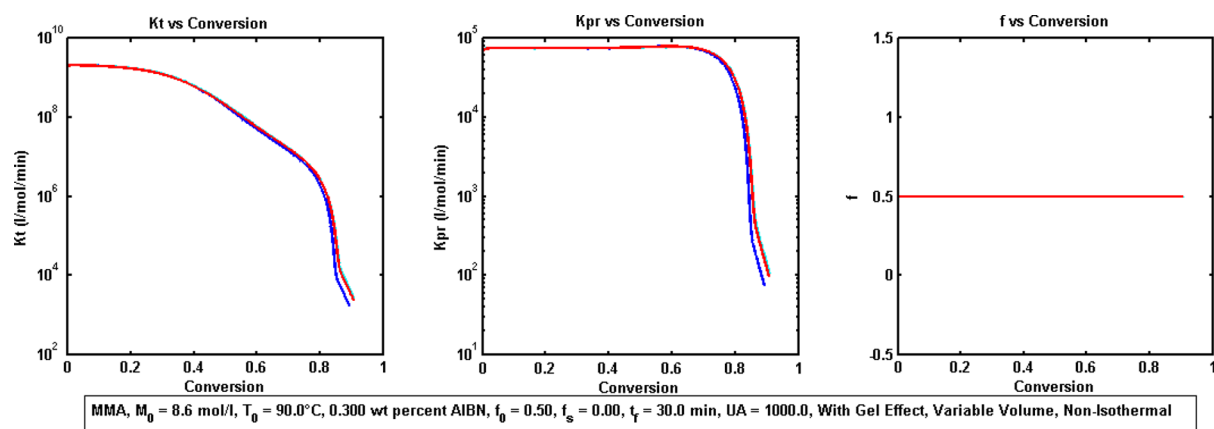
MMA, M_0 = 8.6 mol/l, T_0 = 90.0°C, 0.300 wt percent AIBN, f_0 = 0.50, f_s = 0.00, t_f = 30.0 min, UA = 1000.0, With Gel Effect, Variable Volume, Non-Isothermal

Figure 5. MMA: Results obtained for K_t and K_{pr} for temperature variation with UA = 1000 cal/min/K for the gel/glass effect with the CCS model.
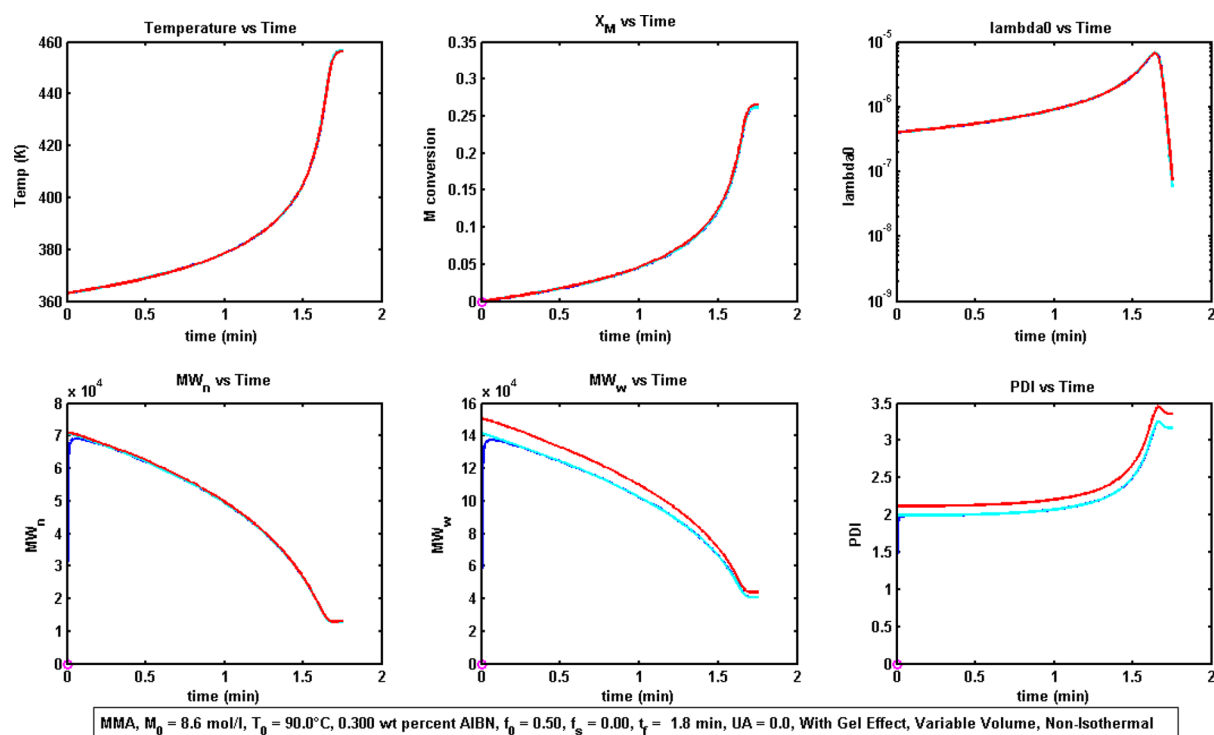

MMA, M_0 = 8.6 mol/l, T_0 = 90.0°C, 0.300 wt percent AIBN, f_0 = 0.50, f_s = 0.00, t_f = 1.8 min, UA = 0.0, With Gel Effect, Variable Volume, Non-Isothermal

Figure 6. MMA: Results obtained for temperature variation with UA = 0 cal/min/K (adiabatic) for the gel/glass effect with the CCS model.

MMA, M_0 = 8.6 mol/l, T_0 = 90.0°C, 0.300 wt percent AIBN, f_0 = 0.50, f_s = 0.00, t_f = 1.8 min, UA = 0.0, With Gel Effect, Variable Volume, Non-Isothermal
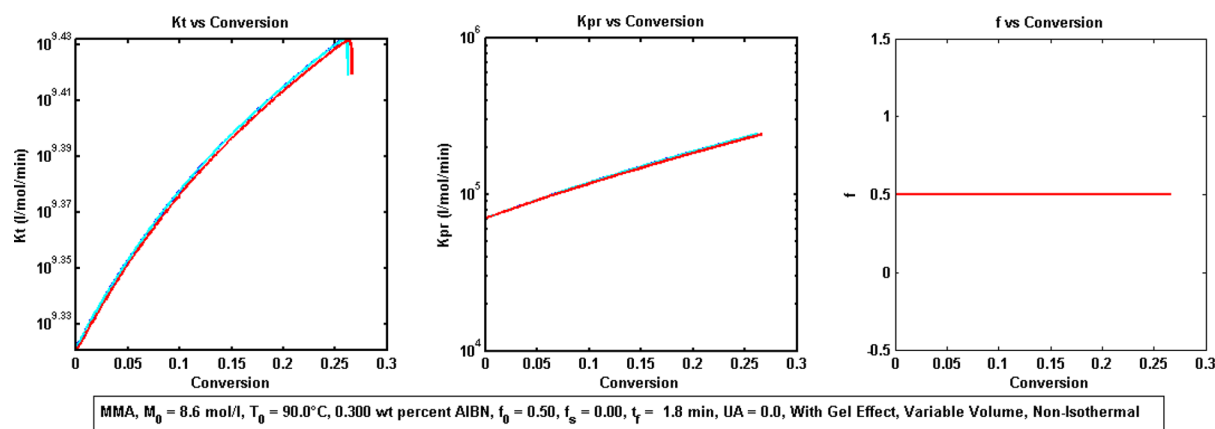
Figure 7. MMA: Results obtained for K_t and K_{pr} for temperature variation with UA = 0 cal/min/K (adiabatic) for gel/glass effect with CCS model.
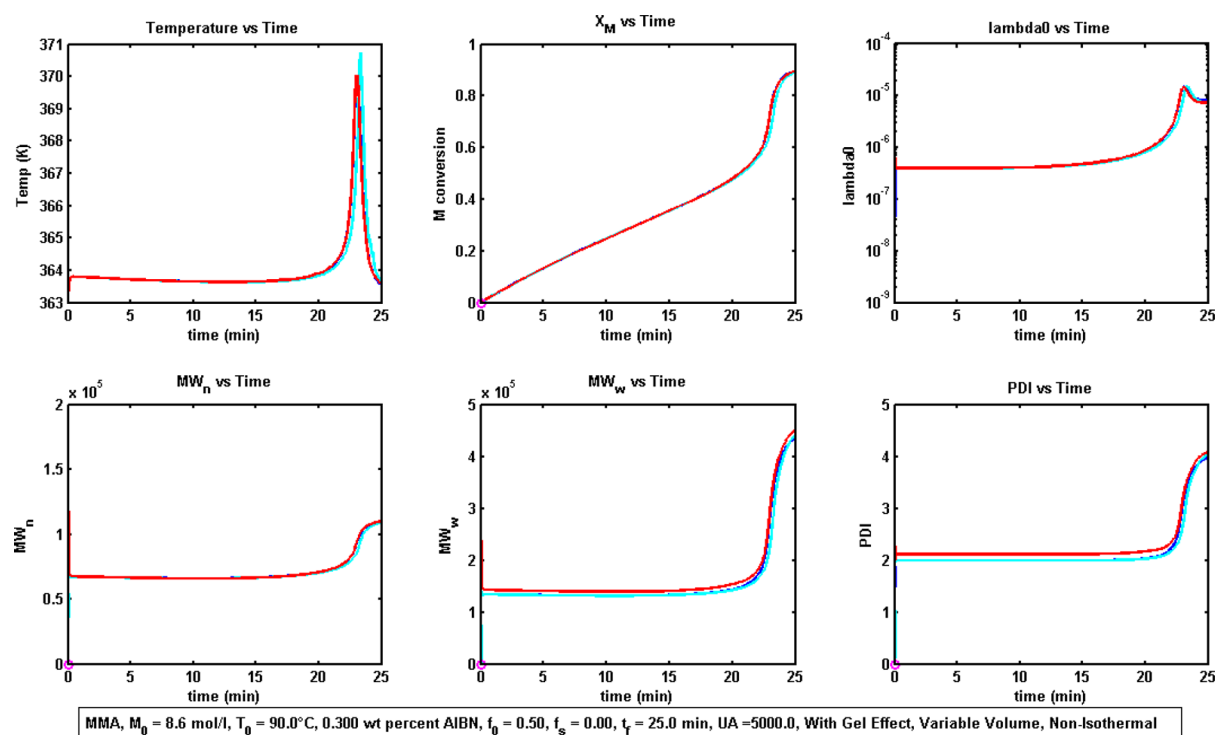
Figure 8. MMA: Results obtained for temperature variation with UA = 5000 cal/min/K with the gel/glass/cage effect using the AK model.
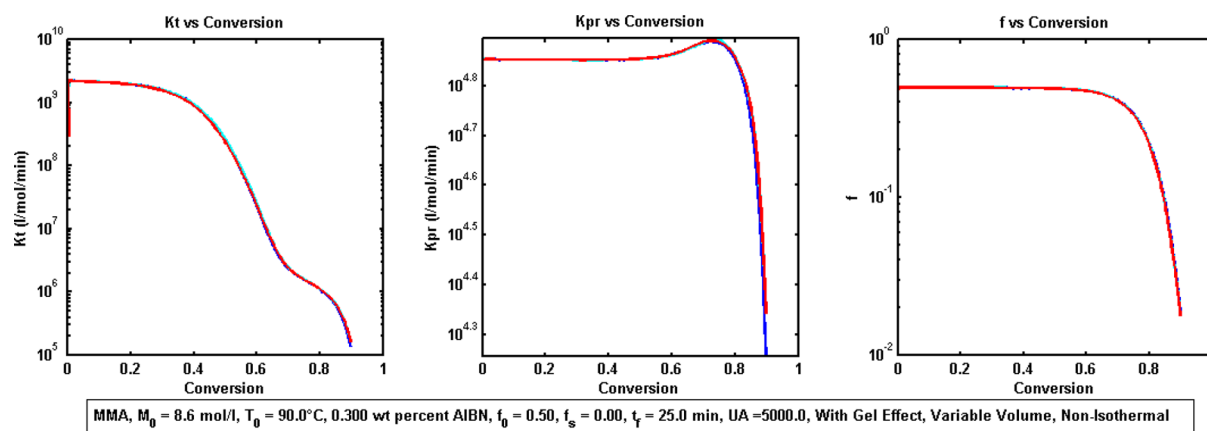

Figure 9. MMA: Results obtained for K_t, K_{pr}, and f for temperature variation with UA = 5000 cal/min/K with the gel/glass/cage effect using the AK model.

■ DISCUSSION

All the nonisothermal results shown here are for three different cases from the complexity point of view of using AS, namely (1) without any gel/glass/cage effect, (2) with the gel/glass effect using the CCS model and, (3) with the gel/glass and cage effect using the AK model. Case 1 here represents AS in its original form[14] and the conditions represent situations before gel effect or under large dilution with solvent leading to no gel effect. Case 2[15] and case 3[16] represent higher conversion cases, and their major differences arise from the complexity of modeling of diffusion coefficients for monomer, polymer and initiator. This affects the prediction of MW_w and PDI as shown in our previous work.[14−16] Most of similar work under non-isothermal condition as reported in the literature was accomplished using CCS model whereas this is probably the first time that AK model (using free volume theory) is being used to show nonisothermal results. It can be seen that the

results of NS matched quite well with AS as well as with each other in all the figures shown. However, different heat transfer rates lead to different situations in terms of reactor temperature profile and parameters value and are discussed in the following. The particular adiabatic effect in all three aforementioned cases is discussed together later.

Figures 1 and 2 show the results for case 1 mentioned above. In Figures 1 and 2, UA decreases from 1000 to 500 cal/min/K. It can be observed that the temperature maxima increases with a decrease in the heat transfer rate, which is about 4 °C in Figure 1 and about 11 °C in Figure 2. This can be explained as follows: as the exothermic polymerization reaction takes place, heat is generated; due to the limitation of heat transfer rate, not all the heat that is generated gets removed. So the remaining heat stays within the system and increases its temperature. This has positive feedback on various kinetic rate coefficients and the rate of reaction is increased, leading to a further increase of heat
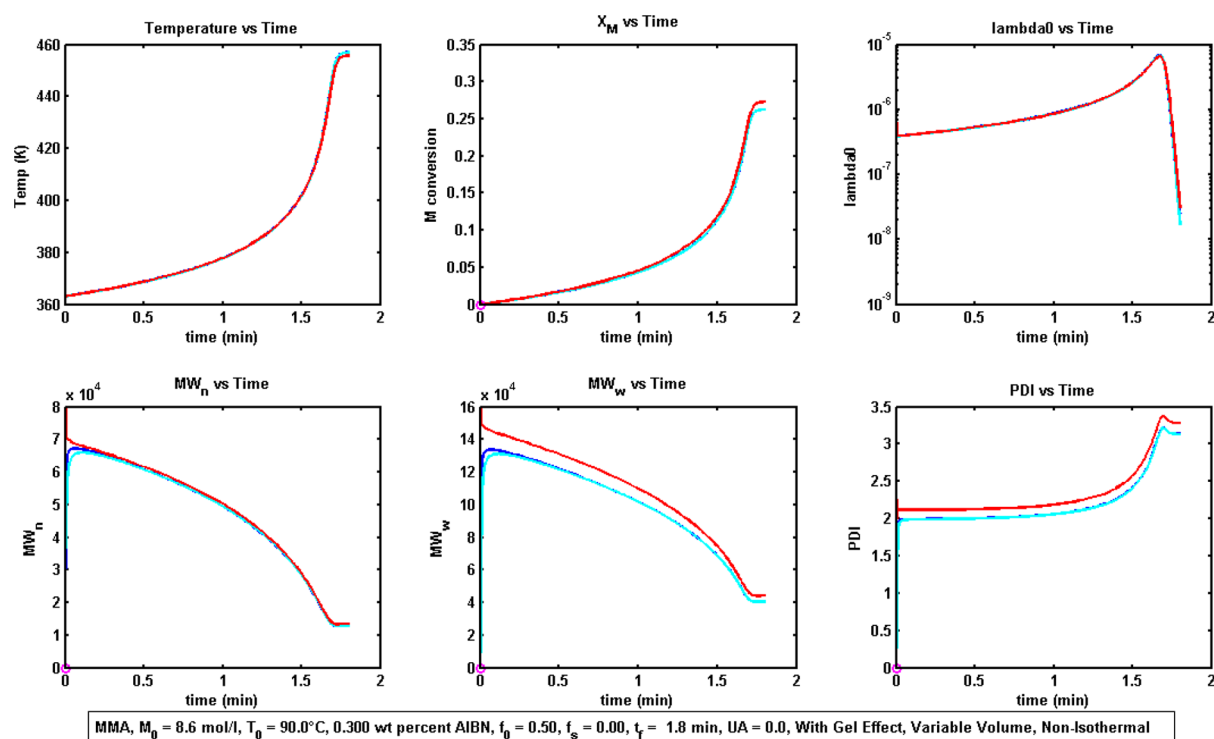
Figure 10. MMA: Results obtained for temperature variation with $UA = 0$ cal/min/K (adiabatic) with the gel/glass/cage effect using the AK model.
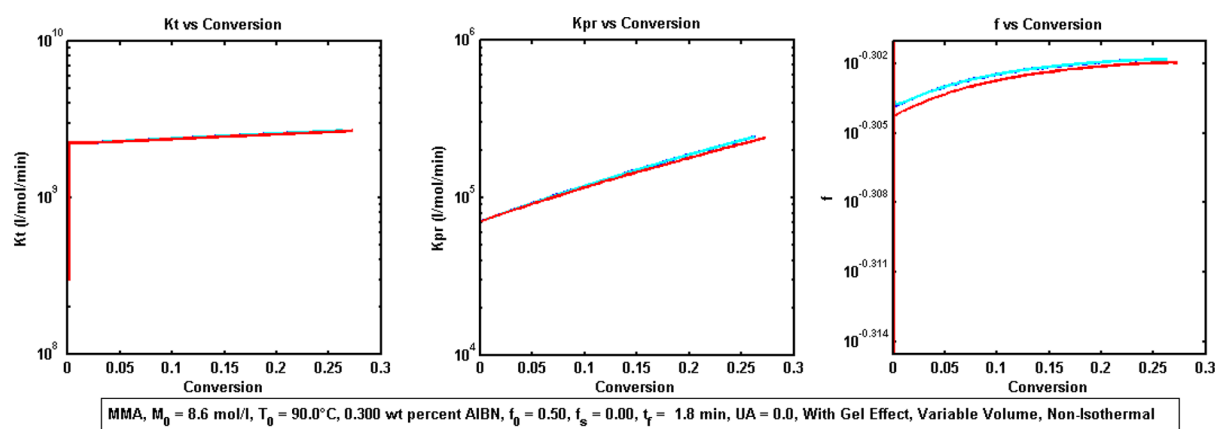

Figure 11. MMA:` obtained for K_t, K_{pr}, and f for temperature variation with $UA = 0$ cal/min/K (adiabatic) with the gel/glass/cage effect using the AK model.

generation, and this in turn further increases the temperature and this cycle goes on. Meanwhile, due to increasing temperature, heat transfer rate is also increased due to an increased thermal gradient. So at a particular temperature, heat removal rate is balanced by heat generation rate. This arrests any further rise in system temperature. Besides this, as the reaction proceeds, the decrease in monomer concentration starts dominating. This decreases the rate of reaction thus decreases the heat of generation. Depending on the actual decrease in rate of reaction, one can observe either the steep fall in system temperature (Figure 2) or very slow fall (Figure 1). This continues until the conversion reaches to a level (whose actual value depending on system conditions) where the gel effect takes place.

To that extent, auto acceleration of the reaction takes place due to decrease in radical termination process which is due to the decrease in the mobility of polymer chains. As a consequence, reaction rate increases quite fast thus increasing the

heat generation again. This, in the absence of proper heat transfer, increases the temperature of the system until it balances out with the heat removal rate. Thus, the temperature profile can have two maxima: one at beginning and another during gel effect. After gel effect, rate of reaction decreases quite rapidly due to the considerable decrease in monomer concentration and due to the increasing glass effect which slows down the reaction to the point where it just freezes. So in the absence of any further heat generation, the system temperature falls finally to heat sink temperature. Since no gel effect is modeled in case 1 here, so we would not be able to observe this effect on temperature profile here. The effect of temperature is almost proportional on molecular weight distribution, higher in Figure 2 compared to that in Figure 1. PDI is at about 2 in both figures, signifying the increased importance of termination by disproportionation over termination by combination. PDI remains nearly constant as the

variation in temperature is not very large, and the effects on MW_n and MW_w are synchronized in such a way that the ratio remains constant.

Figures 4–7 show the results for case 2 as mentioned above. Here, in Figures 4 and 5, the results for finite heat transfer rate, UA = 1000 cal/min/K, are shown whereas Figures 6 and 7 show the results for the adiabatic condition. It can be seen that due to implementing the gel effect, the temperature rise is much higher compared to case 1 without the gel effect. Besides this, it can be observed that there are two temperature maxima compared to case 1 (without gel effect), as already discussed. Baillagou and Soong[1,8] had made a similar observation with the same CCS model. They explained it by stating that the first maximum was due to degenerated runaway. The authors assumed that heat transfer was not sufficient enough to remove produced heat and thus could not prevent the temperature rise initially. But with an increase in temperature, the heat transfer rate also increased (proportional to the difference between T and T_{bath}) and thus this increased heat transfer rate was able to maintain and even lower the temperature a little bit. The second maximum was due to the gel effect as explained earlier. Baillagou and Soong[1,8] had not shown the K_t and K_{pr} profiles which are shown here. The fall in K_t can be observed in Figure 5, leading to the gel effect. K_{pr} can also be observed in the same Figure 5 going to low values, thus leading to the glass effect as shown in Figure 4. That is why the conversion almost became steady.

The profiles for MW_n and PDI are also similar to one obtained by Baillagou and Soong.[8] We can observe that increase in temperature has a negative impact on both MW_n and MW_w, whereas the increase in conversion has a positive one. Initially, MW_n decreases due to increase in temperature but then rises slowly due to increasing conversion and then increases rapidly due tothe dominant impact of increased reaction/conversion during the gel effect over increasing reaction temperature. Then, it falls down a little with the beginning of the glass effect and decreasing temperature. The same happens with MW_w. As an overall consequence, PDI suddenly jumps a little during the gel effect and then increases slowly with time.

Figures 8-11 show the results for case 3 mentioned above, i.e., implementing the gel/glass/cage effect using the AK model. Figures 8 and 9 show the results for UA = 5000 cal/min/K, which is higher compared to the previous cases considered. The results are slightly different compared to Figures 4 and 5 as explained above. The reason for the delayed gel effect is that because of higher the heat transfer rate, the temperature rise is less and thus the conversion rate is lower compared to the case of UA = 1000 cal/min/K. Thus, it takes more time to reach the conversion to cause the gel effect. Besides this, the temperature rise is also less during the gel effect due to the higher heat transfer rate. After reaching the maxima during the gel effect, the temperature now starts falling down due to two reasons: (1) increased temperature increases the temperature gradient to the heat sink thus increasing the heat transfer rate and (2) a decrease in reaction rate due to a decrease in monomer concentration thus producing less thermal energy. This, in a synergetic effect with increasing viscosity due to higher conversion, decreases K_{pr} sharply, thus inducing the glass effect. Unlike Figure 5, in Figure 9, K_t and K_{pr} profiles are different a little bit. K_t is more in line with the prediction of Buback.[18] K_{pr}, here, increases during the gel effect instead of remaining constant probably because of the increased temperature. Unlike

the previous case of constant initiator efficiency in the CCS model, f decreases almost with K_{pr} as predicted by Zhu et al.[19]

Since the temperature before the gel effect remains almost constant so no negative effect of the temperature rise is seen on MW_n and MW_w and thus on PDI; they all remain flat, rising only during the gel effect. PDI reaches a much higher value compared to the low heat transfer rate case as shown in Figure 4. As shown in our previous work, the AK model is better than CCS model for predicting MW_w and thus PDI. So it might be the case that the CCS model in Figure 4 is underestimating PDI.

Figures 3, 6, and 10 represent the situation where adiabatic conditions apply for each of the three cases mentioned above. Sufficiently before the gel effect, all three cases should have the same results and the adiabatic condition is one such situation. Looking carefully, we will observe that all three are the same. The results are the same for Figures 7 and 11. The temperature profile also matches qualitatively with the experimental results obtained by Tonoyan et al.[20] under similar but not quite exact conditions for MMA. This validates the mathematical formulation for each case indirectly. So now we can discuss any one of these figures without referring to all of them separately. There are several important aspects to be noted from the results. In Figure 10, the conversion graph shows that the final conversion is at about 0.26 for the adiabatic condition, which is quite low despite a high temperature. This can easily be explained by the fact that due to such a large temperature rise and that too in such a short time (about 1.6 min) the initiator rapidly decomposes, leading to its complete dissociation, thus leaving a large amount of monomer unreacted. This condition is defined as dead end by Baillagou and Soong.[1] The low conversion combined with high temperature rise leads to an increase in K_t and K_{pr}. The PDI increase is higher than that in the case of finite heat transfer, due to the large production of macroradicals upon initiator decomposition, which favors termination reactions. MW_n and PDI profiles are similar to the ones presented by Baillagou and Soong.[8] Hence we have validated our results under similar conditions.

■ CONCLUSION

The results through Figures 1–11 clearly show that AS results match well with NS for all cases of different heat transfer rates as well as different models for the gel/glass/cage effect. NS also matches with each other for all these conditions. These results clearly establish that the derived AS is extremely flexible, versatile, and adaptable and is as useful as the previous work by Venkateshwaran et al.[13] AS has proved its capability to be used in all practical situations using various models to simulate the gel/glass/cage effect explicitly for covering the complete range of conversion. So instead of using 11 differential equations (eqs A1−A12), only one differential equation (eq A12) is required to be solved using AS for the nonisothermal condition and none for the isothermal condition. This all can be done without any loss of accuracy compared to detailed NS except perhaps at low temperature. NS has also shown to give similar results under all conditions despite the difference in implementing QSSA for eqs A6-A8 in FRP_QSSA compare to FRP_Full. Therefore, one can implement AS only or possibly FRP_QSSA instead of FRP_Full in CFD problems, thus reducing the number of variables to be solved and thus saving simulation time.

■ ASSOCIATED CONTENT

S Supporting Information

Appendix A, mathematical model for free radical polymerization as used in this work, Appendix B, summary of AS in time step format for variable volume condition, Appendix C, constitutive equations for the gel and glass effect using CCS model, Appendix D, constitutive equations for the cage, gel and glass effect using free volume theory, and Appendix E, physical and chemical data. The material is available free of charge via the Internet at http://pubs.acs.org.

■ AUTHOR INFORMATION

Corresponding Author

*(C.A.S). E-mail: ca.serra@unistra.fr.

Notes

The authors declare no competing financial interest.

■ ACKNOWLEDGMENTS

■ NOTATION

A chain transfer agent concentration at any time t, mol/L

A_1 a parameter of the CCS model

A_H area for heat transfer, m^2

A_s proportionality parameter; $A_{s,L}$, $A_{s,U}$, $A_{s,avg}$ are lower, upper, and average values, respectively

B_1 a parameter of the CCS model

B_{n-1} $((8f[K_{pr}]^2 I_{n-1})/(K_d K_t))^{1/2}$, constant in AS at the beginning of the $(n-1)$th time step

C_1 a parameter of the CCS model

C_A K_{fa}/K_p, dimensionless

C_b bulk monomer concentration, mol/L

C_M K_{fm}/K_p, dimensionless

C_{n-1} $2B_{n-1}([V_R]_{n-1}/[V_R]_0)^{1/2}$, constant in AS at the beginning of the $(n-1)$th time step

C_p specific heat capacity of mixture, cal/g/°C

C_S K_{fs}/K_p, dimensionless

C_T K_{td}/K_{tc}, dimensionless

D_{eff} effective diffusion coefficient, m^2/s

D_{i0} pre-exponential factor of diffusion coefficient of chemical species i (i = M, P, I), cm^2/s

D_i diffusion coefficient of chemical species i (i = M, P, I), cm^2/s

D_{n-1} $((2(K_{pr}M_{n-1})^2)/(K_t K_d))e^{-C_{n-1}}$, constant in AS at the beginning of the $(n-1)$th time step

DP_n number-averaged degree of polymerization

E_{d0} activation energy for dissociation rate constant, cal/mol

F_{seg} probability of two radicals to react when their active centers come into close proximity

I initiator concentration, mol/L

K_{MH} Mark−Houwink constant, dL/g

K_d dissociation rate coefficient, min^{-1}

K_{d0} pre-exponential factor of K_d, dissociation rate coefficient, min^{-1}

K_{fa} transfer to CTA rate coefficient, L/(mol·min)

K_{fm} transfer to monomer rate coefficient, L/(mol·min)

K_{fs} transfer to solvent rate coefficient, L/(mol·min)

K_i kinetic rate constant for initiation, s^{-1}

K_p propagation rate coefficient, L/(mol·min)

K_p^0 propagation rate coefficient at time t = 0, L/(mol·min)

K_{pr} $K_p + K_{fm}$ = $(1 + C_M)K_p$, L/(mol·min)

K_t $K_{tc} + K_{td}$, L/(mol·min)

K_t^0 termination rate coefficient at time t = 0, L/(mol·min)

K_{tc} termination by combination rate coefficient, L/(mol·min)

K_{td} termination by disproportionation rate coefficient, L/(mol·min)

$K_{t,res}$ residual termination rate constant, L/(mol·min)

L kinetic chain length, $((K_p M \lambda_0)/(2f K_d I))$

$\overline{L}$ $L(1 - R_{MM})/(1 + R_P L)$ = $L(1 - R_M)/(1 + R_P L)$

M monomer concentration, mol/L

M_{ji} molecular weight of jumping unit of chemical species I (i = M, P, S, I), g/mol

MW   molecular weight, g/mol

MW_n number-averaged chain length of polymer, g/mol

MW_w weight-averaged chain length of polymer, g/mol

N_A Avogadro's constant, 6.023×10^{23} mol^{-1}

P $(2/(R_L + 1)) + (R_T/(R_L + 1)^2)$, parameter in AS

PDI   polydispersity index, dimensionless

P_n dead polymer chain length of n no. of monomer units

R universal gas constant, 1.986 cal/mol/K

R_0 zero order radical obtained from initiator dissociation

R_A $C_A/(1 + C_M) = K_{fa}/K_{pr}$

R_{AM} $C_A/(1 + C_M)(A/M) \approx C_A/(1+C_M)\cdot(A_0/M_0)$

R_H hydrodynamic radius of polymer

R_L $R_P L$, parameter in AS

R_M $(K_{fm}/(K_p + K_{fm}))$ = (K_{fm}/K_{pr}) = $(C_M/(1 + C_M))$

R_{MM} R_M

R_n live polymer chain length of n no. of monomer units

R_P $R_{MM} + R_{SM} + R_{AM}$ = $R_{MM} + R_{SA}$

R_S $(C_s/(1 + C_M))$ = (K_{fs}/K_{pr})

R_{SA} $R_{SM} + R_{AM}$

R_{SM} $(C_s/(1 + C_M))(S/M) \approx (C_S/(1 + C_M))(S_0/M_0)$

R_T $(K_{tc}/(K_{tc} + K_{td}))$ = (K_{tc}/K_t) = $(1/(1 + C_T))$, dimensionless

S solvent concentration any time t, mol/L

T temperature, K

T' $T - T_{bath}$, K

T_{bath} temperature of heat sink, K

T_{gi} glass temperature of chemical species i (i = M, P, S, I), K

U overall heat transfer coefficient, W/m^2/K

V_m monomer volume, cm^3

V_f free volume, dimensionless

V_i^* specific critical hole free volume of species i (i = M, P, S, I), cm^3/g

V_R volume of solution at any time t, L

V_{R0} initial volume of solution at t_0, L

X_{C0} critical degree of polymerization for entanglement of pure polymer

a_{MH} Mark−Houwink constant, dimensionless

a_{seg} parameter depending on initiator type and mixture composition

f initiator efficiency, dimensionless

f_s solvent volume fraction, dimensionless

j_c entanglement spacing between polymer chains

k_B Boltzmann constant, 1.3806×10^{-23} J/K

r_1, r_2 effective reaction radius, cm

r_e Kuhn's segment length, A°

r_m, r_t radius of reaction between polymer radical and monomer

t time, min

x_M monomer conversion, dimensionless

y $e^{((-K_d t)/2)}$, variable evaluated in AS

ΔH_P heat of reaction, cal/mol

β ratio of solvent volume to nonsolvent volume, dimensionless

ε volume contraction factor corrected for solvent volume fraction, dimensionless

ε_0 volume contraction factor without solvent volume fraction, dimensionless

ε_i K_{i0}/K_{p0}

λ_0 zeroth order moment for live polymer chain concentration, mol/L

λ_1 first order moment for live polymer chain concentration, mol/L

λ_2 second order moment for live polymer chain concentration, mol/L

μ_0 zeroth order moment for dead polymer chain concentration, mol/L

μ_1 first order moment for dead polymer chain concentration, mol/L

μ_2 second order moment for dead polymer chain concentration, mol/L

ρ mixture density, g/cm^3

Φ volume fraction, dimensionless

Θ_t parameter defined for gel effect in CCS model

Θ_p parameter defined for glass effect in CCS model

δ average root-mean-square end-to-end distance of polymer chain, A$^\circ$

η_M dynamic viscosity of monomer, cP

$[\eta]$ intrinsic viscosity of the polymer, dL/g

σ Lennard-Jones radius, A$^\circ$

γ overlap factor, dimensionless

ω weight fraction, dimensionless

ξ_{iP} ratio of the critical molar volume of the jumping unit of chemical species i to the critical molar volume of the polymer

τ characteristic time

Subscript

M monomer

P polymer

S solvent

I initiator

n at the beginning of the nth time step

0 at time $t = 0$

■ REFERENCES

(1) Baillagou, P. E.; Soong, D. S. Major Factors Contributing to The Nonlinear Kinetics of Free-Radical Polymerization. *Chem. Eng. Sci.* **1985**, *40* (1), 75−86.

(2) Balke, S. T.; Hamielec, A. E. Bulk Polymerization of Methyl Methacrylate. *J. Appl. Polym. Sci.* **1973**, *17*, 905−949.

(3) Marten, F. L.; Hamielec, A. E. High-Conversion Diffusion-Controlled Polymerization of Styrene. I. *J. Appl. Polym. Sci.* **1982**, *27* (2), 489−505.

(4) McKenna, T. F.; Villanueva, A.; Santos, A. M. Effect of Solvent on The Rate Constants in Solution Polymerization. Part I. Butyl Acrylate. *J. Polym. Sci., Polym. Chem.* **1999**, *37* (5), 571−588.

(5) McKenna, T. F.; Villanueva, A. Effect of Solvent on The Rate Constants in Solution Polymerization. Part II. Vinyl Acetate. *J. Polym. Sci., Polym. Chem.* **1999**, *37* (5), 589−601.

(6) Achilias, D. S.; Kiparissides, C. Development of a General Mathematical Framework for Modeling Diffusion-Controlled Free-Radical Polymerization Reactions. *Macromolecules* **1992**, *25* (14), 3739−3750.

(7) Keramopoulos, A.; Kiparissides, C. Development of a Comprehensive Model for Diffusion-Controlled Free-Radical Copolymerization Reactions. *Macromolecules* **2002**, *35* (10), 4155−4166.

(8) Baillagou, P. E.; Soong, D. S. Molecular-Weight Distribution of Products of Free-Radical Non-Isothermal Polymerization with Gel Effect - Simulation for Polymerization of Poly(Methyl Methacrylate). *Chem. Eng. Sci.* **1985**, *40* (1), 87−104.

(9) Chiu, W. Y.; Carratt, G. M.; Soong, D. S. A Computer-Model for The Gel Effect in Free-Radical Polymerization. *Macromolecules* **1983**, *16* (3), 348−357.

(10) Ray, A. B.; Saraf, D. N.; Gupta, S. K. Free-Radical Polymerizations Associated with The Trommsdorff Effect Under Semibatch Reactor Conditions.I. Modeling. *Polym. Eng. Sci.* **1995**, *35* (16), 1290−1299.

(11) Srinivas, T.; Sivakumar, S.; Gupta, S. K.; Saraf, D. N. Free Radical Polymerizations Associated with The Trommsdorff Effect Under Semibatch Reactor Conditions.II. Experimental Responses to Step Changes in Temperature. *Polym. Eng. Sci.* **1996**, *36* (3), 311−321.

(12) Sangwai, J. S.; Bhat, S. A.; Gupta, S.; Saraf, D. N.; Gupta, S. K. Bulk Free Radical Polymerizations of Methyl Methacrylate Under Non-isothermal Conditions and With Intermediate Addition of Initiator: Experiments and Modeling. *Polymer* **2005**, *46* (25), 11451−11462.

(13) Venkateshwaran, G.; Kumar, A. Solution of Free-Radical Polymerization. *J. Appl. Polym. Sci.* **1992**, *45* (2), 187−215.

(14) Garg, D. K.; Serra, C. A.; Hoarau, Y.; Parida, D.; Bouquey, M.; Muller, R. Analytical Solution of Free Radical Polymerization: Derivation and Validation. *Macromolecules* **2014**, *47* (14), 4567−4586.

(15) Garg, D. K.; Serra, C. A.; Hoarau, Y.; Parida, D.; Bouquey, M.; Muller, R. Analytical Solution of Free Radical Polymerization: Applications-Implementing Gel Effect Using CCS Model. *Macromolecules* **2014**, DOI: 10.1021/ma501251j.

(16) Garg, D. K.; Serra, C. A.; Hoarau, Y.; Parida, D.; Bouquey, M.; Muller, R. Analytical Solution of Free Radical Polymerization: Applications-Implementing Gel Effect Using AK Model. *Macromolecules* **2014**, DOI: 10.1021/ma501413m.

(17) Achilias, D.; Kiparissides, C. Modeling of Diffusion-Controlled Free-Radical Polymerization Reactions. *J. Appl. Polym. Sci.* **1988**, *35* (5), 1303−1323.

(18) Buback, M. Free-Radical Polymerization up to High Conversion - A General Kinetic Treatment. *Makromol. Chem.* **1990**, *191* (7), 1575−1587.

(19) Zhu, S.; Tian, Y.; Hamielec, A. E.; Eaton, D. R. Radical Concentrations in Free-Radical Copolymerization of MMA/EGDMA. *Polymer* **1990**, *31* (1), 154−159.

(20) Tonoyan, A. O.; Leikin, A. D.; Davtyan, S. P.; Rozenberg, B. A.; Yenikolopyan, N. S. Kinetics of The Adiabatic Polymerization of Methyl Methacrylate. *Vysokomol. Soyed.* **1973**, *A15* (8), 1847−1851.